THE JOURNAL OF BIOLOGICAL CHEMISTRY
Vol. 276, No. 24, Issue of June 15, pp. 21425–21433, 2001

Printed in U.S.A.

Caveolin-3 Null Mice Show a Loss of Caveolae, Changes in the Microdomain Distribution of the Dystrophin-Glycoprotein Complex, and T-tubule Abnormalities*

Received for publication, January 29, 2001
Published, JBC Papers in Press, March 19, 2001, DOI 10.1074/jbc.M100828200

Ferruccio Galbiati,[a,b,c,d,e] Jeffrey A. Engelman,[a,b,d] Daniela Volonte,[a,b,e] Xiao Lan Zhang,[a,b] Carlo Minetti,[f,g] Maomi Li,[h] Harry Hou, Jr.[i] Burkhard Kneitz,[i] Winfried Edelmann,[i,j] and Michael P. Lisanti,[a,b,k]

From the [a]Departments of Molecular Pharmacology, [h]Pathology, and [i]Cell Biology and the [b]Albert Einstein Comprehensive Cancer Center, Albert Einstein College of Medicine, Bronx, New York 10461 and the [f]Servizio Malattie Neuro-Muscolari, Università di Genova, Istituto Gaslini, Largo Gaslini 5, 16147 Genova, Italy

Caveolin-3, a muscle-specific caveolin-related protein, is the principal structural protein of caveolae membrane domains in striated muscle cells. Recently, we identified a novel autosomal dominant form of limb-girdle muscular dystrophy (LGMD-1C) in humans that is due to mutations within the coding sequence of the human caveolin-3 gene (3p25). These LGMD-1C mutations lead to an ~95% reduction in caveolin-3 protein expression, *i.e.* a caveolin-3 deficiency. Here, we created a caveolin-3 null (CAV3 −/−) mouse model, using standard homologous recombination techniques, to mimic a caveolin-3 deficiency. We show that these mice lack caveolin-3 protein expression and sarcolemmal caveolae membranes. In addition, analysis of skeletal muscle tissue from these caveolin-3 null mice reveals: (i) mild myopathic changes; (ii) an exclusion of the dystrophin-glycoprotein complex from lipid raft domains; and (iii) abnormalities in the organization of the T-tubule system, with dilated and longitudinally oriented T-tubules. These results have clear mechanistic implications for understanding the pathogenesis of LGMD-1C at a molecular level.

Caveolae are 50–100-nm vesicular invaginations of the plasma membrane that participate in vesicular trafficking events and signal transduction processes (1–5). Caveolin, a 21–24-kDa integral membrane protein, is a principal component of caveolae membranes *in vivo* (6–10). Caveolin is only the first member of a new gene family; as a consequence, caveolin has been re-termed caveolin-1 (11).

The mammalian caveolin gene family now consists of caveolin-1, -2, and -3 (3, 11–13). Caveolin-1 and -2 are co-expressed and form a hetero-oligomeric complex (14) in many cell types, with particularly high levels in adipocytes, whereas expression of caveolin-3 is muscle-specific and found in both cardiac and skeletal muscle, as well as smooth muscle cells (15). Expression of caveolin-3 is induced during the differentiation of skeletal myoblasts, and caveolin-3 is localized to the muscle cell plasma membrane (sarcolemma), where it forms a complex with dystrophin and its associated glycoproteins (15). It has been proposed that caveolin family members function as scaffolding proteins (16) to organize and concentrate specific lipids (cholesterol and glycosphingolipids; Refs. 17–19) and lipid modified signaling molecules (Src-like kinases, Ha-Ras, endothelial nitric-oxide synthase, and G-proteins; Refs. 17 and 20–24) within caveolae membranes.

Caveolin-3 is most closely related to caveolin-1 based on protein sequence homology; caveolin-1 and caveolin-3 are ~65% identical and ~85% similar (13). However, caveolin-3 mRNA is expressed predominantly in muscle tissue types (skeletal muscle, diaphragm, and heart) (13). Identification of a muscle-specific member of the caveolin gene family has implications for understanding the role of caveolins in different muscle cell types, as previous morphological studies have demonstrated that caveolae are abundant in these cells. This indicates that muscle cell caveolae may play an important role in muscle membrane biology.

Tight regulation of caveolin-3 expression appears essential for maintaining normal muscle homeostasis, as we have demonstrated that transgenic overexpression of wild-type (WT)[1] caveolin-3 in mouse skeletal muscle fibers induces a Duchenne-like muscular dystrophy phenotype (25). Analysis of skeletal muscle tissue from transgenic mice overexpressing caveolin-3 revealed: (i) a dramatic increase in sarcolemmal caveolae; (ii) hypertrophic, necrotic, and regenerating skeletal muscle fibers with central nuclei; and (iii) down-regulation of dystrophin and β-dystroglycan protein expression.

One possibility is that overexpression of wild-type caveolin-3 disrupts the normal processing or stoichiometry of the dystro-

* This work was supported in part by grants from the National Institutes of Health, the Muscular Dystrophy Association, the American Heart Association, and the Susan B. Komen Breast Cancer Foundation (to M. P. L.). The costs of publication of this article were defrayed in part by the payment of page charges. This article must therefore be hereby marked "*advertisement*" in accordance with 18 U.S.C. Section 1734 solely to indicate this fact.

[c] Recipient of Fellowship 470/bi from Telethon-Italia. Current address: The University of Pittsburgh School of Medicine, Dept. of Pharmacology, Biomedical Science Tower East, Rm. 1302, Pittsburgh, PA 15261-0001.

[d] These authors contributed equally to this work.

[e] Current address: The University of Pittsburgh School of Medicine, Dept. of Pharmacology, Biomedical Science Tower East, Rm. 1356, Pittsburgh, PA 15261-0001.

[g] Supported by grants from Telethon-Italia and the Italian Ministry of Health (G. Gaslini Institute, Ricerca Finalizzata).

[j] Supported by National Institutes of Health Grant R01-CA-76329.

[k] Recipient of a Hirsch/Weil-Caulier Career Scientist Award. To whom correspondence should be addressed: Albert Einstein College of Medicine, 1300 Morris Park Ave., Bronx, NY 10461. Tel.: 718-430-8828; Fax: 718-430-8830; E-mail: lisanti@aecom.yu.edu.

[1] The abbreviations used are: WT, wild-type; LGMD, limb-girdle muscular dystrophy; K/O band, knockout band; KO mice, knockout mice; mAb, monoclonal antibody; kb, kilobase pair(s); TBST, Tris-buffered saline with Tween 20; Mes, 4-morpholineethanesulfonic acid; PBS, phosphate-buffered saline; PAGE, polyacrylamide gel electrophoresis; RyR, ryanodine receptor; DHPR, dihydropyridine receptor.

phin complex, leading to its degradation. In support of this hypothesis, we have recently demonstrated that a novel WW-like domain within caveolin-3 directly recognizes the extreme C terminus of β-dystroglycan that contains a PP*X*Y motif (26). As the WW domain of dystrophin recognizes the same site within β-dystroglycan, caveolin-3 can effectively block the interaction of dystrophin with β-dystroglycan *in vitro* (26), suggesting competitive regulation of the recruitment of dystrophin to the sarcolemma *in vivo*.

In collaboration with Minetti and colleagues (27), we have identified an autosomal dominant form of limb-girdle muscular dystrophy (LGMD-1C) in two Italian families that is due to a deficiency in caveolin-3 expression. Analysis of their genomic DNA reveals two distinct mutations in caveolin-3: (i) a 9-base pair microdeletion that removes the sequence TFT from the caveolin scaffolding domain, and (ii) a missense mutation that changes a proline to a leucine (Pro → Leu) in the transmembrane domain (27). Both mutations lead to a loss of ~90–95% of caveolin-3 protein expression.

Using heterologous expression in cultured cells, we have recently demonstrated that LGMD-1C mutants of caveolin-3 behave in a dominant-negative fashion, causing the intracellular retention and degradation of wild-type caveolin-3 via the proteasome system (28). Interestingly, treatment with proteasomal inhibitors blocks the dominant negative effect of LGMD-1C mutants and rescues wild-type caveolin-3 (29).

Here, using a gene targeting approach, we generated mice lacking caveolin-3 protein expression (CAV3 −/−). Analysis of skeletal muscle fibers from these caveolin-3 null mice reveals mild myopathic changes, with a loss of sarcolemmal caveolae, that is consistent with what is observed in patients with LGMD-1C. In addition, skeletal muscle fibers from these caveolin-3 null mice are characterized by alterations in targeting of the dystrophin-glycoprotein complex to lipid raft microdomains and abnormalities in the organization of the T-tubule system. These data suggest that mislocalization of the dystrophin complex and abnormal T-tubule development may underlie the pathogenesis of LGMD-1C in humans.

EXPERIMENTAL PROCEDURES

Materials—Antibodies and their sources were as follows: anti-caveolin-3 IgG (mAb 26 (15); gift of Dr. Roberto Campos-Gonzalez, Transduction Laboratories, Inc.); anti-caveolin-1 IgG (mAb 2297 (30); gift of Dr. Roberto Campos-Gonzalez); anti-caveolin-2 IgG (mAb 65 (14); gift of Dr. Roberto Campos-Gonzalez); anti-β-dystroglycan IgG (mAb, NCL-b-DG; Novocastra, Newcastle, United Kingdom); anti-α-sarcoglycan (mAb, NCL-a-SARC; Novocastra); anti-dystrophin IgG (mAb, NCL-DYS3; Novocastra); anti-DHPR-1α IgG (for immunofluorescence, polyclonal antibody DHPR-1α N19 (Santa Cruz Biotechnology); for Western blotting, mAb DHPR-1α D-218 (Sigma)); anti-ryanodine-R IgG (for immunofluorescence, polyclonal antibody RyR N19 (Santa Cruz Biotechnology); for Western blotting, mAb RyR R-129 (Sigma)). All other biochemicals used were of the highest purity available and were obtained from regular commercial sources.

Assembly of the Caveolin-3 Construct for Targeted Gene Disruption—Briefly, an ~200-kb BAC clone containing murine caveolin-3 was previously isolated using the murine caveolin-3 cDNA as a probe for colony hybridizations (31). An 8-kb *Bam*HI subclone containing the second exon of caveolin-3 was isolated and cloned into the *Bam*HI site of Bluescript (pBS SK+). This was used for the 3′ end of the construct. From this clone, a 4.0-kb *Xba*I/*Bgl*II fragment was isolated and cloned into pCB7. This fragment was isolated by double digestion with *Xba*I and *Sac*I and cloned into the PGT-N29 vector (New England Biolabs, Inc.) that contains the neomycin resistance gene. From the original BAC clone, a 10-kb *Kpn*I subclone was isolated and cloned into Bluescript (pBS SK+). This clone contains exon 2 of caveolin-3 and was used for the 5′ end of the construct. An internal 4.4-kb *Bam*HI fragment was subcloned into Bluescript, which then was liberated with *Eco*RI (yielding a 4.2-kb fragment) and subcloned into pGT-N29 that already possessed the 3′ end of the construct. The final knockout construct was linearized with *Xho*I.

Derivation of ES Cell Clones Harboring a Disrupted Caveolin-3 Gene—After electroporation of the WW6 ES cell line (gift of Dr. Pamela Stanley) with the linearized DNA containing the caveolin-3 K/O construct, G418-resistant clones were selected for analysis. Homologous recombination was detected by Southern blot analysis. Genomic DNA from approximately 1000 G418-resistant ES cell clones was prepared. For each clone, ~10 μg of genomic DNA was digested with *Eco*RI and separated on an 0.8% agarose gel. The DNA was transferred to nitrocellulose and probed with a 1.5-kb *Bgl*II fragment that is 3′ to the knockout construct. Homologous recombination was detected by the presence of a ~8.5-kb band (K/O band) in addition to a ~13-kb band (WT band). This is due to the introduction of an additional *Eco*RI site into the caveolin-3 locus via homologous recombination (see Fig. 1).

Generation of Caveolin-3 Knock-out Mice—We injected positive ES cell clones into blastocysts in order to obtain chimeric mice with germline transmission of the caveolin-3 gene disruption. We next backcrossed the resulting heterozygote mice at least three times with C57BL/6 mice (Jackson Laboratories). Homozygous null mice were identified by Southern blot analysis by the presence of the ~8.5-kb band (K/O band) and the absence of the ~13-kb band (WT band). In addition, homozygous mice were identified by PCR analysis using primers specific for the neomycin resistance gene and exon-2 of caveolin-3. Amplification of only the neomycin resistance gene, but not caveolin-3/exon-2, indicated that the mice were homozygous null. CAV3 +/+ (WT) and CAV3 −/− (caveolin-3 null) mice comprising the F_4 generation were subjected to detailed analysis. For all experiments described herein, each experiment was repeated at least twice, and four mice were analyzed in a given experimental group. Animals were analyzed at 8–12 weeks of age; however, virtually identical results were also obtained with 6-month-old mice.

Immunoblot Analysis—Mouse tissues were harvested, minced with a scissors, homogenized in a Polytron tissue grinder for 30 s at a medium range speed, and solubilized in a buffer containing 10 mM Tris-HCl (pH 8.0), 150 mM NaCl, 5 mM EDTA, 1% Triton X-100, and 60 mM octyl glucoside for 45 min at 4 °C. In addition, samples were centrifuged at 13,000 × *g* for 10 min at 4 °C to remove insoluble proteins. Soluble proteins were resolved by SDS-PAGE (12.5% or 8% acrylamide) and transferred to BA83 nitrocellulose membranes (0.2 μm, Schleicher & Schuell). Blots were incubated for 2 h in TBST (10 mM Tris-HCl, pH 8.0, 150 mM NaCl, 0, 2% Tween 20) containing 2% powdered skim milk and 1% bovine serum albumin. After three washes with TBST, membranes were incubated for 2 h with the primary antibody (~1,000-fold diluted in TBST) and for 1 h with horseradish peroxidase-conjugated goat anti-rabbit/mouse IgG (~5,000-fold diluted). Bound antibodies were detected using an ECL detection kit (Amersham Pharmacia Biotech).

Histological and Histochemical Analyses—Muscle tissue sections were subjected to hematoxylin/eosin staining, essentially as described (32).

Immunostaining of Murine Skeletal Muscle Tissue Sections—Samples were isolated from the extensor digitorum longus, the soleus, and the gastrocnemius muscle, rapidly frozen in liquid nitrogen-cooled isopentane, sectioned, and stored in liquid nitrogen. Unfixed serial sections (4 μm thick) of frozen muscle were incubated with a given primary antibody for 1 h at room temperature (~1000-fold diluted in PBS with 0.1% Triton X-100, 0.2% bovine serum albumin). After three washes with PBS (10 min each), sections were incubated with the secondary antibody for 1 h at room temperature: lissamine rhodamine B sulfonyl chloride-conjugated goat anti-rabbit antibody (5 μg/ml)/fluorescein isothiocyanate-conjugated goat anti-mouse antibody (5 μg/ml). Finally, the sections were washed three times with PBS (10 min each wash), and slides were mounted with Slow-Fade anti-fade reagent (Molecular Probes, Inc., Eugene, OR) and observed under a Bio-Rad MR 600 confocal microscope. Three-dimensional reconstructions were performed using National Institutes of Health Image software.

Transmission Electron Microscopy—Mouse skeletal muscle tissue samples were fixed with glutaraldehyde, post-fixed with OsO_4, and stained with uranyl acetate and lead citrate. Samples were examined under a JEOL 1200EX transmission electron microscope and photographed (magnification, ×25,000) (33–35). Caveolae were identified by their characteristic flask shape, size (50–100 nm), and location at or near the plasma membrane (36).

T-tubule System Staining—T-tubule system staining was performed as described previously (37). Briefly, mouse skeletal muscle tissue samples were fixed in 2% paraformaldehyde, 2.5% glutaraldehyde, 0.1 M cacodylate, and 50 mM $CaCl_2$, pH 7.4. Samples were post-fixed with 2% OsO_4, 0.8% $K_3Fe(CN)_6$, followed by incubation with saturated uranyl acetate. Samples were dehydrated in a graded series of ethanol and embedded in LX112 (Ladd Research Industries). Sections were cut on Reichert UCT ultramicrotome and examined under a JEOL 1200EX

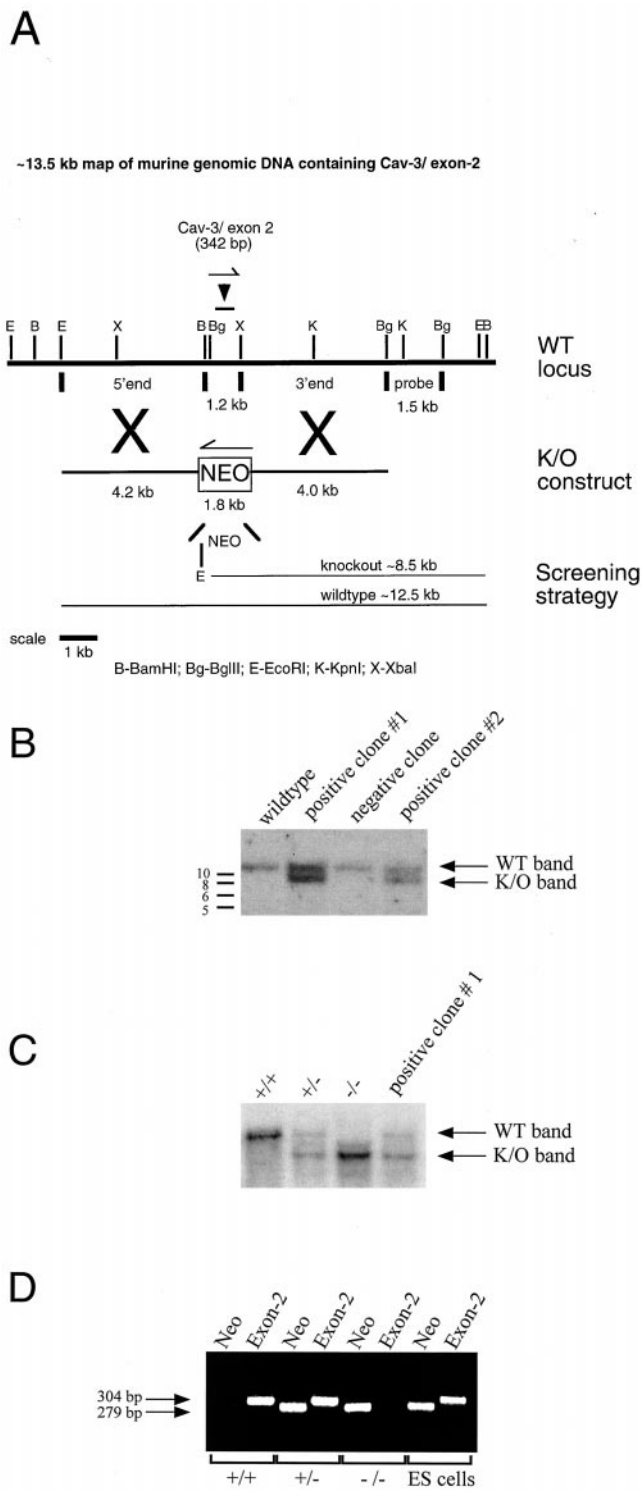

FIG. 1. **Generating caveolin-3 null (CAV3 −/−) mice via homologous recombination.** *A*, generation of the caveolin-3 construct for targeted gene disruption. The knockout construct for murine caveolin-3 was designed to replace exon-2 of caveolin-3 with the neomycin resistance gene cassette, but in the opposite transcriptional orientation. A BAC clone containing murine caveolin-3 was previously isolated using the murine caveolin-3 cDNA as a probe for colony hybridizations and its intron/exon organization was determined (31). An 8-kb *Bam*HI subclone containing the second exon of caveolin-3 was isolated and cloned into the *Bam*HI site of Bluescript (pBS SK+). It was used for the 3′ end of the construct. From this clone, a 4.0-kb *Xba*I/*Bgl*II fragment was isolated and cloned into pCB7. This fragment was then isolated by double digestion with *Xba*I and *Sac*I and cloned into the PGT-N29 vector (New England Biolabs, Inc.) that contains the neomycin resistance gene. From the original BAC clone, a 10-kb *Kpn*I subclone was isolated and cloned into Bluescript (pBS SK+). This clone contained exon 2 of caveolin-3 and was used for the 5′ end of the construct. An internal 4.4-kb *Bam*HI fragment was subcloned into Bluescript, which was then liberated with *Eco*RI (yielding a 4.2-kb fragment) and subcloned into pGT-N29 that already possessed the 3′ end of the construct. The final knockout construct was linearized with *Xho*I. *B*, derivation of ES cell clones harboring a disrupted caveolin-3 gene. After electroporation of the WW6 ES cell line (38) with the linearized DNA containing the caveolin-3 K/O construct, G418-resistant clones were selected for analysis. Homologous recombination was detected by Southern blot analysis. Genomic DNA from approximately 1000 G418-resistant ES cell clones was prepared. For each clone, ~10 μg of genomic DNA was digested with *Eco*RI and separated on a 0.8% agarose gel. The DNA was transferred to nitrocellulose and probed with a 1.5-kb *Bgl*II fragment that is 3′ to the knockout construct (Fig. 1*A*). Homologous recombination was detected in several independent clones by the presence of a ~8.5-kb band (K/O band) in addition to a ~13-kb band (WT band). This is due to the introduction of an additional *Eco*RI site into the caveolin-3 locus via homologous recombination (see *panel A*). *C*, identification of homozygous null mice harboring a disrupted caveolin-3 gene by Southern blot analysis. Positive clones were injected into blastocysts in order to obtain chimeric mice with germline transmission of this caveolin-3 gene disruption. We next crossed the resulting heterozygote mice to obtain homozygote mice that harbored the intended gene disruption. Approximately 10 μg of genomic DNA was extracted from mouse tail biopsies, digested with *Eco*RI, and separated on a 0.8% agarose gel. The DNA was transferred to nitrocellulose and probed with a 1.5-kb *Bgl*II fragment that is 3′ to the knockout construct. Homozygous null mice were identified by the presence of the ~8.5-kb band (K/O band) and the absence of the ~13-kb band (WT band). *D*, identification of homozygous null mice harboring a disrupted caveolin-3 gene by PCR analysis. In addition, homozygous null mice were identified by PCR analysis using primers specific for the neomycin resistance gene and exon-2 of caveolin-3. Amplification of only the neomycin resistance gene, but not caveolin-3/exon2, indicated that the mice were homozygous null. *bp*, base pairs.

transmission electron microscope and photographed (magnification, ×12,000).

Preparation of Caveolae-enriched Membrane Fractions—Mouse skeletal muscle tissue was harvested, minced with a scissors, and homogenized in 2 ml of Mes-buffered saline containing 1% (v/v) Triton X-100. Homogenization was carried out with a Polytron tissue grinder for 30 s at a medium range speed at 4 °C. Samples were centrifuged at low speed for 5 min at 4 °C, and the supernatant was adjusted to 40% sucrose by the addition of 2 ml of 80% sucrose prepared in Mes-buffered saline and placed at the bottom of an ultracentrifuge tube. A 5–30% linear sucrose gradient was formed above the homogenate and centrifuged at 39,000 rpm for 16–20 h in a SW41 rotor (Beckman Instruments). A light scattering band confined to the 15–20% sucrose region was observed that contained endogenous caveolin-3, but excluded most of other cellular proteins. From the top of each gradient, 1-ml gradient fractions were collected to yield a total of 12 fractions. An equal amount of protein from each gradient fraction was separated by SDS-PAGE and subjected to immunoblot analysis.

RESULTS

Generating Caveolin-3 Null Mice via Homologous Recombination—A BAC clone containing murine caveolin-3 was previously isolated using the murine caveolin-3 cDNA as a probe for colony hybridizations, and its intron/exon organization was determined; the caveolin-3 gene consists of only two coding exons (31). The knockout construct for murine caveolin-3 was designed to replace exon-2 of caveolin-3 with the neomycin resistance gene cassette, but in the opposite transcriptional orientation (Fig. 1*A*). Importantly, exon-2 of caveolin-3 encodes the bulk of the caveolin-3 protein and all of its functional domains (13, 31).

After electroporation of the WW6 ES cell line (38) with the linearized DNA containing the caveolin-3 K/O construct, G418-resistant clones were selected for analysis. Homologous recombination was detected by Southern blot analysis (Fig. 1*B*). Next, positive clones were injected into blastocysts in order to obtain chimeric mice with germline transmission of this caveolin-3 gene disruption. We next crossed the resulting heterozygote mice (CAV3 +/−) to obtain homozygote mice (CAV3 −/−)

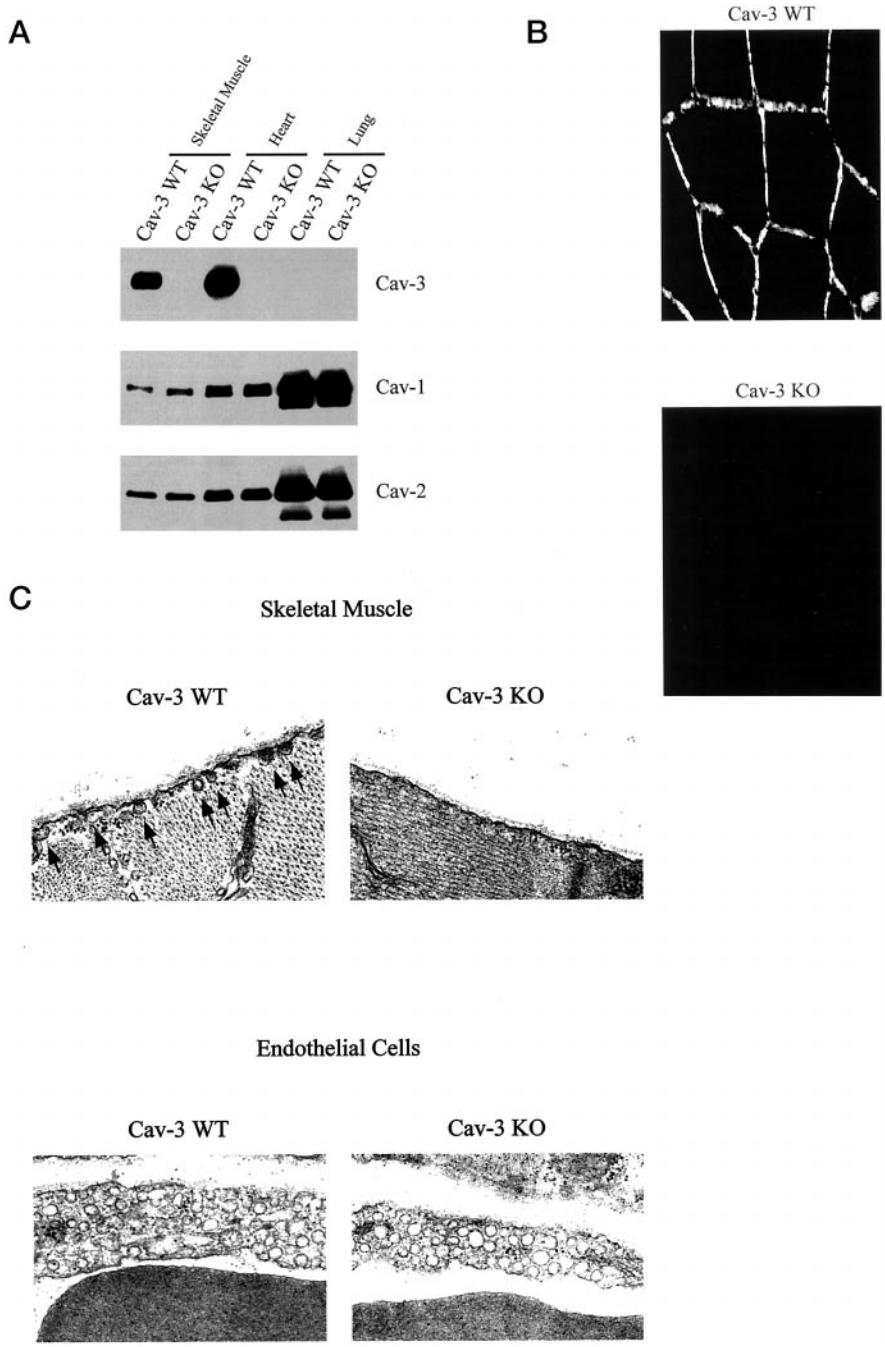

FIG. 2. **Caveolin-3 null mice do not express the caveolin-3 protein and lack sarcolemmal caveolae.** *A*, Western blot analysis. Protein lysates were prepared from skeletal muscle, heart, and lung tissues of WT mice and caveolin-3 KO mice. After SDS-PAGE and transfer to nitrocellulose, immunoblotting was performed with monospecific antibodies probes that recognize only caveolin-1, caveolin-2, or caveolin-3. Note that caveolin-3 is only expressed in skeletal muscle and in the heart of WT mice. Interestingly, caveolin-1 and -2 are equally expressed in WT mice and caveolin-3 null mice. The presence of caveolin-1 and -2 in skeletal muscle and cardiac tissues reflects their expression in fibroblasts, endothelial cells, and smooth muscle cells, but caveolin-1 and -2 are not expressed in the striated muscle cells themselves (14, 15). Each lane contains an equal amount of total protein. *B*, immunocytochemistry. Skeletal muscle tissue sections were prepared from WT mice (*upper panel*) and caveolin-3 KO mice (*lower panel*). After immunostaining with antibodies directed against caveolin-3, samples were observed under a confocal microscope. Note that caveolin-3 is expressed only in WT mice. *C*, transmission electron microscopy analysis. Transmission electron micrographs of skeletal muscle cells (*upper panels*) and neighboring endothelial cells (*lower panels*) from WT mice (*left panels*) and caveolin-3 KO mice (*right panels*) are shown. Note that a lack of caveolin-3 expression in caveolin-3 KO mice results in an absence of caveolae at the sarcolemma (muscle cell plasma membrane). As expected, caveolae are still present in endothelial cells from WT mice and caveolin-3 KO mice.

that harbored the intended gene disruption.

Homozygous null mice were identified by the presence of the ~8.5-kb band (K/O band) and the absence of the ~13-kb band (WT band) on Southern blots (Fig. 1*C*). In addition, homozygous null mice were identified by PCR analysis using primers specific for the neomycin resistance gene and exon-2 of caveolin-3. Amplification of only the neomycin resistance gene, but not caveolin-3/exon2, indicated that the mice were homozygous null (Fig. 1*D*).

CAV3 (−/−) Mice Do Not Express the Caveolin-3 Protein Product and Lack Sarcolemmal Caveolae Membrane Domains—To demonstrate the loss of caveolin-3 protein expression, tissues were harvested from WT and caveolin-3 null mice and examined by Western blot analysis using a caveolin-3 specific mAb probe. In all cases, CAV3 +/− mice were crossed and the resulting CAV3 +/+ and CAV3 −/− littermates were compared. Fig. 2*A* shows that caveolin-3 is only expressed in skeletal muscle and heart tissues from WT mice, but is clearly absent in caveolin-3 null mice. In contrast, the expression of caveolin-1 and -2, the other members of the caveolin gene family, was not affected in caveolin-3 null mice.

As the first exon of caveolin-3 was not removed by our recombination strategy, we also analyzed the possible expression of Cav-3/exon-1 in these mice. Cav-3/exon-1 (114 base pairs) is predicted to encode a truncated protein that contains residues 1–38 of caveolin-3, which do not contain any of the known functional domains of the caveolins. All of the functional domains of caveolin-3 are contained within exon-2 (residues 39–151), which has been replaced by our cloning strategy. Importantly, the monospecific mAb probe we used to detect caveolin-3 protein expression is directed against the unique N terminus of caveolin-3 (residues 3–24) (15). Therefore, this antibody would recognize a truncated Cav-3/exon-1 protein, if it was expressed. However, smaller truncated forms of the

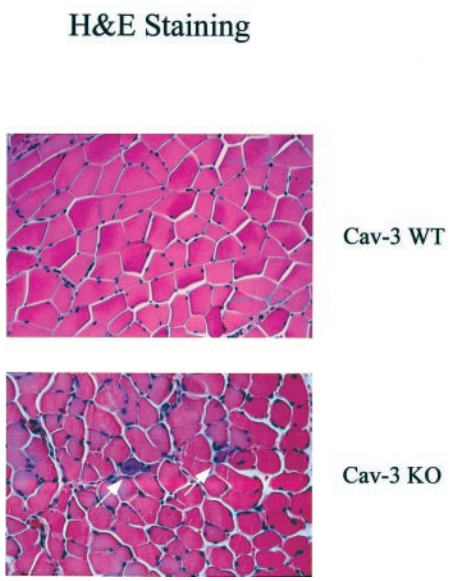

FIG. 3. **Histological analysis of skeletal muscle fibers from caveolin-3 null mice.** Muscle tissue sections from WT mice (*upper panel*) and caveolin-3 KO mice (*lower panel*) were stained with hematoxylin and eosin (*H&E*). Note that muscle tissue sections from caveolin-3 KO mice exhibit variability in muscle fiber size and reveal the presence of some necrotic fibers (see *arrows*).

caveolin-3 protein were not observed.

Next, skeletal muscle tissue sections from WT and caveolin-3 null mice were immunostained with anti-caveolin-3 IgG. Fig. 2*B* shows that caveolin-3 is correctly expressed at the sarcolemma in WT mice, but is clearly absent in caveolin-3 null mice.

Recombinant expression of caveolin-3 in cultured cells is sufficient to drive caveolae formation (39). As caveolin-3 is the only member of the caveolin gene family expressed in striated muscle cells, caveolin-3 is thought to be responsible for caveolae formation in skeletal muscle cells *in vivo*. In fact, transgenic overexpression of caveolin-3 in skeletal muscle fibers dramatically increases the number of plasmalemmal caveolae (25). Thus, we would predict that loss of caveolin-3 expression in caveolin-3 null mice would ablate sarcolemmal caveolae formation.

As predicted, electron microscopic analysis of skeletal muscle fibers revealed an absence of sarcolemmal caveolae in caveolin-3 null mice (Fig. 2*C*, *upper panels*). Importantly, caveolae were still present in endothelial cells from caveolin-3 null mice (Fig. 2*C*, *lower panels*). This is consistent with our previous observations demonstrating that endothelial cells express only caveolin-1 and -2, but not caveolin-3 (14).

Histological Analysis of Muscle Tissues from Caveolin-3 Null Mice Reveals Mild Myopathic Changes—Interestingly, caveolin-3 null mice did not show an overt "clinical" phenotype. In order to identify a phenotype associated with loss of caveolin-3 expression in caveolin-3 null mice, tissue sections from these mice were hematoxylin/eosin-stained and examined by light microscopy. Interestingly, no pathological changes were observed, with the exception of skeletal muscle tissue (Fig. 3; data not shown). Importantly, several pathologists carefully assessed the other tissues (including the heart) where caveolin-3 is endogenously expressed and did not observe any noticeable pathologic changes.

Hematoxylin/eosin staining of skeletal muscle tissue sections from caveolin-3 null mice revealed only mild myopathic changes (Fig. 3). These changes included variability in the size of the muscle fibers and the presence of necrotic fibers. In addition to muscle biopsies, serum creatine kinase levels are used clinically to diagnose muscular dystrophy. As creatine kinase is a cytosolic muscle enzyme, elevated serum creatine kinase levels indicate lysis or necrosis of muscle fibers, with a subsequent release of the enzyme into the blood. Interestingly, caveolin-3 null mice showed sporadic elevations (an ~3–4-fold increase) in serum creatine kinase activity (data not shown), consistent with the skeletal muscle fiber degeneration observed in tissue sections (Fig. 3).

Importantly, the mild muscle damage we observed in the caveolin-3 null mice is very similar to the findings we described earlier for human LGMD-1C, where caveolin-3 expression is reduced by ~90–95% (27). Taken together, these results indicate that a deficiency in caveolin-3 expression (CAV3 −/−) in mice is sufficient to induce a mild myopathic phenotype that is consistent with LGMD-1C in humans.

The Dystrophin-Glycoprotein Complex Is Excluded from Detergent-resistant Membrane Microdomains in Caveolin-3 Null Mice—As caveolin-3 is found associated with dystrophin and dystrophin-associated glycoproteins at the level of the sarcolemma (15, 40), one possibility is that loss of caveolin-3 affects the level of expression and/or the localization of dystrophin and dystrophin-associated glycoproteins. To test this hypothesis, we next examined the level of expression and localization of these proteins in caveolin-3 null mice.

Western blot analysis of lysates prepared from skeletal muscle tissue revealed that caveolin-3 null mice expressed normal levels of dystrophin, α-sarcoglycan, and β-dystroglycan (Fig. 4*A*). Virtually identical results were obtained by immunocytochemistry, indicating that dystrophin, α-sarcoglycan, and β-dystroglycan protein expression is not affected in caveolin-3 null mice (Fig. 4*B*). Interestingly, these proteins were still localized at the sarcolemma in skeletal muscle fibers lacking caveolin-3 expression (Fig. 4*B*). These results are consistent with our previous data showing that the expression level and the macroscopic localization of dystrophin and its associated glycoproteins are not affected by the loss of caveolin-3 expression in human LGMD-1C (27).

We and others have shown previously that dystrophin and its associated glycoproteins co-purify with caveolin-3 and are normally targeted to cholesterol-sphingolipid raft domains/caveolae (15, 26, 40, 41). Next, we evaluated if dystrophin and dystrophin-associated glycoproteins were enriched in cholesterol-sphingolipid-rich raft domains in WT and caveolin-3 null mice. When caveolin-3 is expressed, it is targeted to these lipid rafts and induces the formation of morphological caveolae (39), as caveolins are cholesterol-binding proteins (5, 42). However, cholesterol-sphingolipid rafts exist in the absence of caveolin protein expression (30, 33, 43). Interactions between cholesterol and shingolipids make these plasma membrane microdomains resistant to non-ionic detergents at low temperatures, thereby facilitating their rapid purification (5, 44, 45).

Cholesterol-sphingolipid rafts/caveolae were purified using an established equilibrium sucrose density gradient system that separates these detergent resistant membranes from the bulk of cellular membranes and cytosolic proteins (see "Experimental Procedures") (20, 30, 33, 34, 46–52). In this fractionation scheme, immunoblotting with anti-caveolin-3 IgG can be used to track the position of caveolae-derived membranes within these bottom-loaded sucrose gradients (13, 15). These caveolae-enriched membranes (fractions 4–6) exclude >99.95% of total cellular proteins and also markers for non-caveolar plasma membrane, Golgi, lysosomes, mitochondria, and endoplasmic reticulum (retained in fractions 8–12) (33, 34, 48).

Fig. 4*C* shows that dystrophin, α-sarcoglycan, and β-dystroglycan are all excluded from these cholesterol-sphingolipid raft domains in caveolin-3 null mice. These results indicate that,

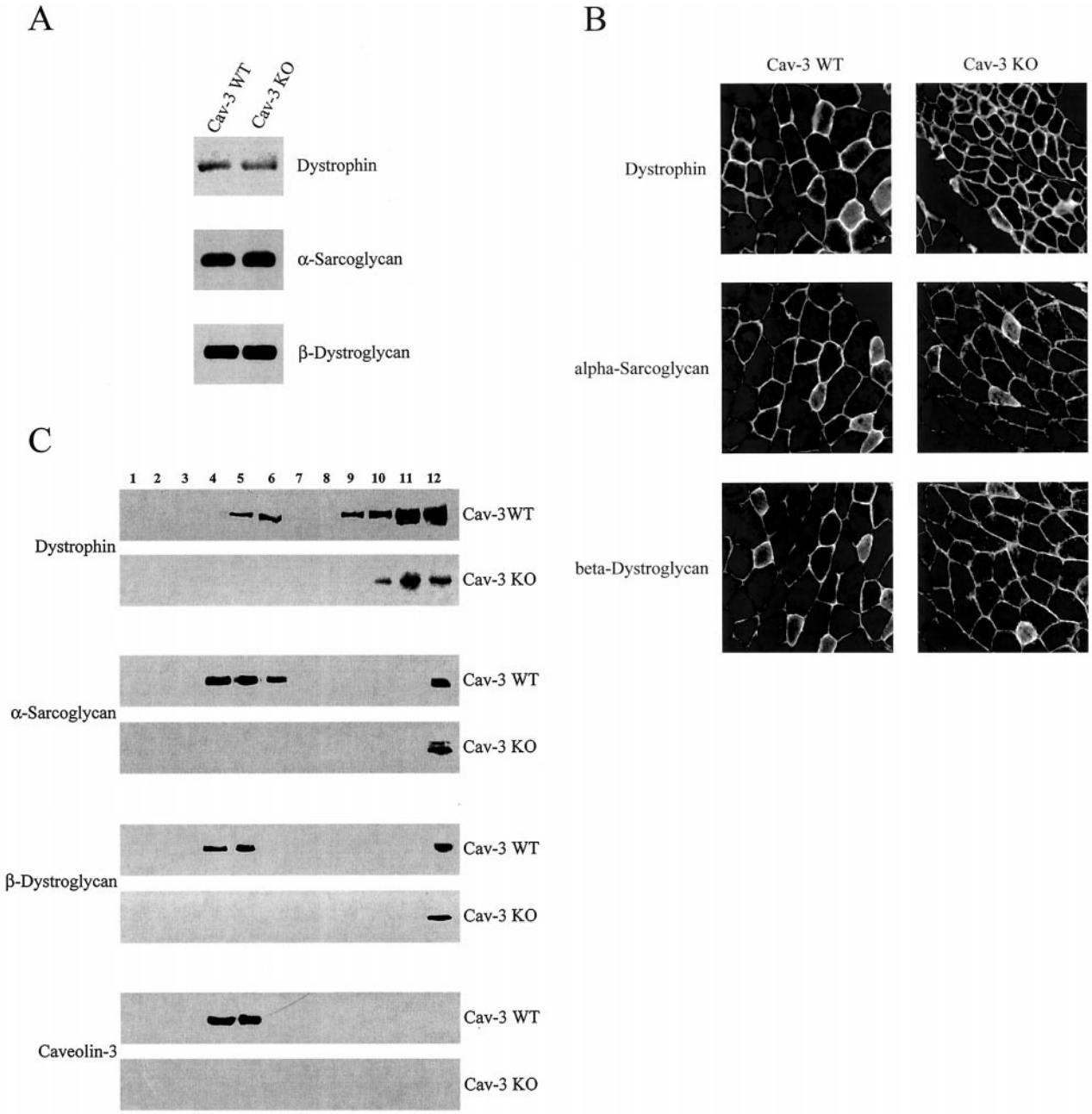

FIG. 4. **Caveolin-3 protein expression is required for the correct targeting of the dystrophin-glycoprotein complex to cholesterol-sphingolipid raft domains/caveolae in normal muscle fibers.** *A*, Western blot analysis. Protein lysates were prepared from skeletal muscle of WT mice and caveolin-3 null mice. After SDS-PAGE and transfer to nitrocellulose, immunoblotting was performed with monospecific antibody probes that recognize dystrophin (*upper panel*), α-sarcoglycan (*middle panel*), and β-dystroglycan (*lower panel*). Note that dystrophin, α-sarcoglycan, and β-dystroglycan are expressed at normal levels in the skeletal muscle of caveolin-3 KO mice. Each lane contains an equal amount of total protein. *B*, immunocytochemistry. Skeletal muscle tissue sections were prepared from WT mice (*left panels*) and caveolin-3 KO mice (*right panels*). After immunostaining with antibodies directed against dystrophin, α-sarcoglycan, and β-dystroglycan, samples were observed under a confocal microscope. Note that dystrophin, α-sarcoglycan, and β-dystroglycan are expressed at normal levels at the plasma membrane in WT mice and caveolin-3 KO mice. *C*, targeting to cholesterol-sphingolipid-rich raft domains/caveolae. Skeletal muscle tissue samples from WT mice and caveolin-3 KO mice were subjected to subcellular fractionation. To separate membranes enriched in lipid rafts/caveolae from the bulk of cellular membranes and cytosolic proteins, an established equilibrium sucrose density gradient system was utilized (see "Experimental Procedures"). In this fractionation scheme, immunoblotting with anti-caveolin IgG can be used to track the position of lipid rafts/caveolae (fractions 4–6) within these bottom-loaded sucrose gradients. Note that dystrophin, α-sarcoglycan, and β-dystroglycan are excluded from lipid raft domains in caveolin-3 KO mice.

although the expression levels of dystrophin and dystrophin-associated glycoproteins do not change in caveolin-3 null mice, their microscopic localization within cholesterol-sphingolipid rafts/caveolae domains is compromised. As the dystrophin-glycoprotein complex is important for normal skeletal muscle functioning, our results suggest that mislocalization of dystrophin, α-sarcoglycan, and β-dystroglycan in caveolin-3 null mice may contribute to the myopathic changes we observe in skeletal muscle tissue sections.

Thus, we conclude that caveolin-3 protein expression is required for the correct targeting of the dystrophin-glycoprotein complex to cholesterol-sphingolipid raft domains/caveolae in normal muscle fibers. These results are consistent with our recent observation that caveolin-3 interacts directly with the dystrophin-glycoprotein complex by recognizing a PP*X*Y motif in the C-terminal tail of β-dystroglycan (26).

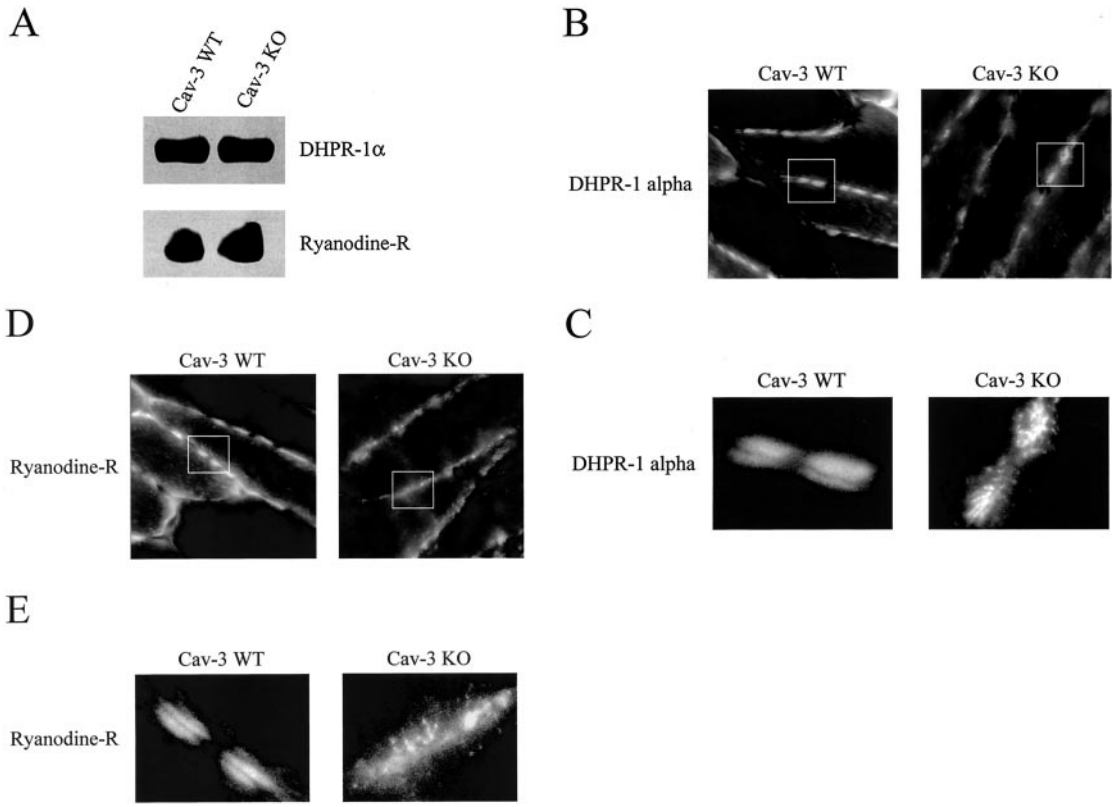

FIG. 5. **Dihydropyridine receptor-1α and ryanodine receptor are expressed at normal levels, but are mislocalized in skeletal muscle fibers from caveolin-3 null mice.** *A*, Western blot analysis. Protein lysates were prepared from skeletal muscle tissue of WT mice and caveolin-3 null mice. After SDS-PAGE and transfer to nitrocellulose, immunoblotting was performed with monospecific antibodies probes that recognize DHPR-1α (*upper panel*) and ryanodine receptor (*Ryanodine-R*) (Lower panel). Note that DHPR-1α and ryanodine receptor are expressed at normal levels in caveolin-3 null mice. Each lane contains an equal amount of total protein. *B–E*, immunocytochemistry. Skeletal muscle tissue sections were prepared from WT mice and caveolin-3 null mice. After immunostaining with antibodies directed against DHPR-1α (*B* and *C*), and ryanodine receptor (*Ryanodine-R*) (*D* and *E*) samples were observed under a confocal microscope. Note that DHPR-1α and ryanodine R show the characteristic double row staining pattern in skeletal muscle fibers from WT mice. However, DHPR-1α and ryanodine R show a more diffuse staining pattern in skeletal muscle fibers from caveolin-3 null mice. The *boxed* areas in *panels B* and *D* are shown at a higher magnification level in *panels C* and *E*, respectively.

Caveolin-3 Deficiency Is Associated with Abnormalities of the T-tubule System—Caveolin-3 has been shown to be transiently associated with the T-tubule system during skeletal muscle development (53). However, it remains unknown whether caveolin-3 expression is required for or greatly facilitates the proper development of the T-tubule system. To test this hypothesis, we analyzed the protein expression and localization of two well known T-tubule markers, dihydropyridine receptor-1α and ryanodine receptor in WT and caveolin-3 null mice. Skeletal muscle tissue lysates from WT and caveolin-3 null mice were subjected to Western blot analysis using monoclonal antibody probes specific for dihydropyridine receptor-1α and ryanodine receptor. Fig. 5*A* shows that the protein expression of these T-tubule markers is not altered in caveolin-3 null mice.

However, the localization of dihydropyridine receptor-1α and ryanodine receptor was severely affected in the skeletal muscle fibers of caveolin-3 null mice. In WT mice, double rows of discrete punctate immunostaining, representing pairs of triads on the opposite sides of the Z-lines, were observed using monoclonal antibody probes specific for dihydropyridine receptor-1α (Fig. 5, *B* and *C*, *left panels*) and ryanodine receptor (Fig. 5, *D* and *E*, *left panels*).

In striking contrast, dihydropyridine receptor-1α (Fig. 5, *B* and *C*, *right panels*) and ryanodine receptor (Fig. 5, *D* and *E*, *right panels*) showed a diffuse pattern of expression in skeletal muscle sections from caveolin-3 null mice. A three-dimensional reconstruction of these sections is shown in Fig. 6. These results suggest that the organization of the T-tubule system is clearly abnormal or immature in caveolin-3 null mice.

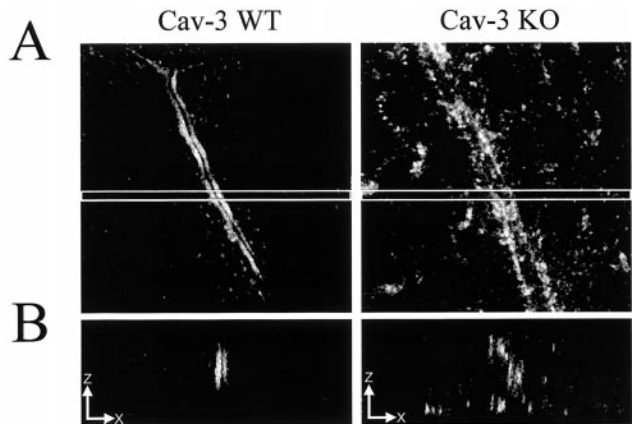

FIG. 6. **Three-dimensional reconstruction of dihydropyridine receptor-1α immunostaining.** *A*, skeletal muscle tissue sections were prepared from WT mice and caveolin-3 KO mice. After immunostaining with antibodies directed against DHPR-1α, Z-series were acquired using a Bio-Rad MR 600 confocal microscope. Images shown represent the three-dimensional reconstructions of 4-μm-thick sections as viewed in the *x-y* plane. *B*, *boxed* regions in *panel A* are also shown as viewed from the *x-z* plane. Note that DHPR-1α is localized diffusely along the length of the muscle fiber in caveolin-3 KO mice, while it is concentrated in discrete double rows in WT mice.

In order to further explore the organization of the T-tubule system in detail, we next employed a well established method

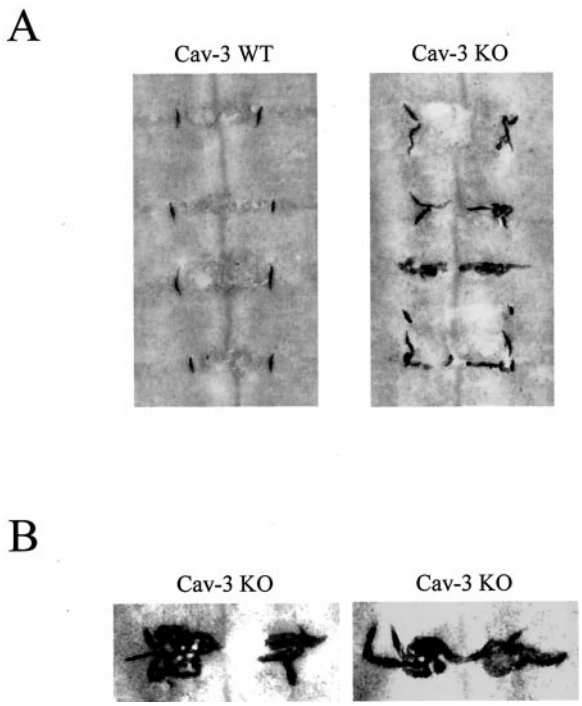

FIG. 7. **Caveolin-3 protein expression is required for the development of a mature highly organized T-tubule system.** Skeletal muscle tissue samples from WT mice (*A*, *left panel*) and caveolin-3 KO mice (*A*, *right panel*) were subjected to T-tubule system staining using potassium ferrocyanate (see "Experimental Procedures"). As a consequence, the T-tubules appear as electron-dense structures (stained *black*). Note that the T-tubule system is dilated and longitudinally oriented in caveolin-3 KO mice. Transmission electron micrographs of skeletal muscle sections from caveolin-3 KO mice are also shown in *panel B* at a higher magnification.

to specifically stain the T-tubule system so that it can be visualized by electron microscopy, *i.e.* the potassium ferrocyanate method (see "Experimental Procedures") (37). Fig. 7*A* shows that T-tubules have an orderly transverse orientation in WT mice (*left panel*), as is expected. However, electron micrographs of the longitudinal sections from caveolin-3 null mice indicate that the T-tubules are dilated/swollen and run in irregular directions (Fig. 7*A*, *right panel*). Transmission electron micrographs at a higher magnification better illustrate the abnormal organization of the T-tubule system in caveolin-3 null mice (Fig. 7*B*). Interestingly, T-tubules in a predominantly longitudinal orientation are typical of immature muscle in normal mice.

DISCUSSION

LGMD-1C is an autosomal dominant form of limb-girdle muscular dystrophy that is genetically caused by mutations within the coding regions of the caveolin-3 gene. In collaboration with Minetti and colleagues (27), we recently identified two different Italian families with this autosomal dominant form of limb-girdle muscular dystrophy that is due to a deficiency in caveolin-3 expression. In these patients, by quantitative immunofluorescence and Western blot analysis, the levels of the caveolin-3 protein were reduced by ~90–95%. Additionally, muscle biopsies from these patients showed muscle damage of mild-to-moderate severity (27).

Here, we created a caveolin-3-deficient (CAV3 −/−) mouse model, using standard homologous recombination techniques, to mimic the situation in patients with LGMD-1C. Importantly, loss of caveolin-3 protein expression resulted in loss of caveolae at the sarcolemma (Fig. 2*C*). This result clearly indicates that caveolin-3 is required for caveolae formation in skeletal muscle cells *in vivo*. Analysis of skeletal muscle tissue from caveolin-3 null mice revealed mild myopathic changes, with variability in the size of the muscle fibers and the presence of necrotic fibers (Fig. 3). Taken together, these results indicate that loss of caveolin-3 and sarcolemmal caveolae is sufficient to induce a mild myopathy that is similar in its severity to that seen in patients with LGMD-1C.

In patients with LGMD-1C, the level of expression and sarcolemma localization of dystrophin and dystrophin-associated glycoproteins is not affected by loss of caveolin-3 expression (27). Similarly, analysis of skeletal muscle fibers from caveolin-3 null mice showed that the expression levels and macroscopic localization of dystrophin, α-sarcoglycan, and β-dystroglycan was not affected (Fig. 4, *A* and *B*).

However, the precise distribution of dystrophin and its associated glycoproteins within the sarcolemma in absence of caveolin-3 protein expression has not been addressed. Here, we demonstrate that dystrophin, α-sarcoglycan, and β-dystroglycan are all excluded from cholesterol-sphingolipid rafts, in the absence of caveolin-3 expression (Fig. 4*C*). Thus, one function of caveolin-3 is to recruit the dystrophin-glycoprotein complex to cholesterol-sphingolipid rafts/caveolae in normal muscle fibers. As dystrophin and dystrophin-associated glycoproteins are important for normal skeletal muscle functioning, these findings suggest a possible mechanism for understanding the pathogenesis of LGMD-1C in humans.

In fully differentiated skeletal muscle fibers, caveolin-3 is associated with sarcolemmal caveolae (53). However, early morphological studies suggested that T-tubules form from the repeated budding of caveolae (37, 54). In addition, caveolin-3 is transiently associated with T-tubules during the differentiation of primary cultured cells and the development of mouse skeletal muscle fibers (53). These results suggest that a functional relationship may exist between caveolin-3 expression, caveolae formation, and T-tubule biogenesis. It remains unknown whether caveolin-3 expression is required for proper T-tubule biogenesis.

Thus, we next assessed the status of the T-tubule system in caveolin-3 null mice. Here, we show that two T-tubule marker proteins (dihydropyridine receptor-1α and ryanodine receptor) are mislocalized in skeletal muscle fibers from caveolin-3 null mice. The localization of these marker proteins also provides an indication that the T-tubule system is disorganized or immature in caveolin-3 null mice (Figs. 5 (*B–E*) and 6).

In accordance with this interpretation, electron micrographs of longitudinal sections from caveolin-3 null mice indicate that the T-tubules are dilated/swollen and run in irregular directions (Fig. 7, *A* and *B*). Interestingly, the T-tubule network has an exclusively longitudinal orientation at early stages of muscle differentiation and only becomes transversely oriented in fully differentiated skeletal muscle fibers (37). As the T-tubule system in caveolin-3 null mice showed a clear tendency to run longitudinally, these results suggest that caveolin-3 expression and caveolae formation are required to generate a highly organized/fully mature T-tubule system *in vivo*. Thus, a disorganized immature T-tubule system may also contribute to the pathogenesis of LGMD-1C in humans.

Acknowledgments—We thank Dr. Frank Macaluso for expertise in T-tubule staining and Jorge Bermudez for help in collecting frozen sections of skeletal muscle tissue.

Addendum—While this work was being completed, another paper appeared describing the generation of caveolin-3 null mice (55). In accordance with our results, these authors demonstrate that loss of caveolin-3 expression prevents caveolae formation and induces a mild myopathy (55), as is known to occur in patients with LGMD-1C (27). However, these authors did not provide any additional mechanistic insights into how caveolin-3 deficiency causes muscular dystrophy. In

contrast, we show here that caveolin-3 expression is required for (i) the proper targeting of the dystrophin-glycoprotein complex to lipid rafts/caveolae and (ii) the development of a highly organized T-tubule system. As the dystrophin-glycoprotein complex and the T-tubule system represent important elements in normal muscle functioning, we speculate that alterations in their organization may contribute to the mild myopathic changes that we observed in caveolin-3 null mice and in patients with LGMD-1C.

REFERENCES

1. Lisanti, M. P., Scherer, P., Tang, Z.-L., and Sargiacomo, M. (1994) *Trends Cell Biol.* **4,** 231–235
2. Couet, J., Li, S., Okamoto, T., Scherer, P. S., and Lisanti, M. P. (1997) *Trends Cardiovasc. Med.* **7,** 103–110
3. Okamoto, T., Schlegel, A., Scherer, P. E., and Lisanti, M. P. (1998) *J. Biol. Chem.* **273,** 5419–5422
4. Engelman, J. A., Zhang, X. L., Galbiati, F., Volonte, D., Sotogia, F., Pestell, R. G., Minetti, C., Scherer, P. E., Okamoto, T., and Lisanti, M. P. (1998) *Am. J. Hum. Genet.* **63,** 1578–1587
5. Smart, E. J., Graf, G. A., McNiven, M. A., Sessa, W. C., Engelman, J. A., Scherer, P. E., Okamoto, T., and Lisanti, M. P. (1999) *Mol. Cell. Biol.* **19,** 7289–304
6. Glenney, J. R., and Soppet, D. (1992) *Proc. Natl. Acad. Sci. U. S. A.* **89,** 10517–10521
7. Glenney, J. R. (1992) *FEBS Lett.* **314,** 45–48
8. Glenney, J. R. (1989) *J. Biol. Chem.* **264,** 20163–20166
9. Rothberg, K. G., Heuser, J. E., Donzell, W. C., Ying, Y., Glenney, J. R., and Anderson, R. G. W. (1992) *Cell* **68,** 673–682
10. Kurzchalia, T., Dupree, P., Parton, R. G., Kellner, R., Virta, H., Lehnert, M., and Simons, K. (1992) *J. Cell Biol.* **118,** 1003–1014
11. Scherer, P. E., Okamoto, T., Chun, M., Nishimoto, I., Lodish, H. F., and Lisanti, M. P. (1996) *Proc. Natl. Acad. Sci. U. S. A.* **93,** 131–135
12. Parton, R. G. (1996) *Curr. Opin. Cell Biol.* **8,** 542–548
13. Tang, Z.-L., Scherer, P. E., Okamoto, T., Song, K., Chu, C., Kohtz, D. S., Nishimoto, I., Lodish, H. F., and Lisanti, M. P. (1996) *J. Biol. Chem.* **271,** 2255–2261
14. Scherer, P. E., Lewis, R. Y., Volonte, D., Engelman, J. A., Galbiati, F., Couet, J., Kohtz, D. S., van Donselaar, E., Peters, P., and Lisanti, M. P. (1997) *J. Biol. Chem.* **272,** 29337–29346
15. Song, K. S., Scherer, P. E., Tang, Z.-L., Okamoto, T., Li, S., Chafel, M., Chu, C., Kohtz, D. S., and Lisanti, M. P. (1996) *J. Biol. Chem.* **271,** 15160–15165
16. Sargiacomo, M., Scherer, P. E., Tang, Z.-L., Kubler, E., Song, K. S., Sanders, M. C., and Lisanti, M. P. (1995) *Proc. Natl. Acad. Sci. U. S. A.* **92,** 9407–9411
17. Li, S., Song, K. S., and Lisanti, M. P. (1996) *J. Biol. Chem.* **271,** 568–573
18. Murata, M., Peranen, J., Schreiner, R., Weiland, F., Kurzchalia, T., and Simons, K. (1995) *Proc. Natl. Acad. Sci. U. S. A.* **92,** 10339–10343
19. Fra, A. M., Masserini, M., Palestini, P., Sonnino, S., and Simons, K. (1995) *FEBS Lett.* **375,** 11–14
20. Li, S., Okamoto, T., Chun, M., Sargiacomo, M., Casanova, J. E., Hansen, S. H., Nishimoto, I., and Lisanti, M. P. (1995) *J. Biol. Chem.* **270,** 15693–15701
21. Song, K. S., Li, S., Okamoto, T., Quilliam, L., Sargiacomo, M., and Lisanti, M. P. (1996) *J. Biol. Chem.* **271,** 9690–9697
22. Li, S., Couet, J., and Lisanti, M. P. (1996) *J. Biol. Chem.* **271,** 29182–29190
23. Shaul, P. W., Smart, E. J., Robinson, L. J., German, Z., Yuhanna, I. S., Ying, Y., Anderson, R. G. W., and Michel, T. (1996) *J. Biol. Chem.* **271,** 6518–6522
24. Garcia-Cardena, G., Oh, P., Liu, J., Schnitzer, J. E., and Sessa, W. C. (1996) *Proc. Natl. Acad. Sci. U. S. A.* **93,** 6448–6453
25. Galbiati, F., Volonte, D., Chu, J. B., Li, M., Fine, S. W., Fu, M., Bermudez, J., Pedemonte, M., Weidenheim, K. M., Pestell, R. G., Minetti, C., and Lisanti, M. P. (2000) *Proc. Natl. Acad. Sci. U. S. A.* **97,** 9689–94
26. Sotgia, F., Lee, J. K., Das, K., Bedford, M., Petrucci, T. C., Macioce, P., Sargiacomo, M., Bricarelli, F. D., Minetti, C., Sudol, M., and Lisanti, M. P. (2000) *J. Biol. Chem.* **275,** 38048–38058
27. Minetti, C., Sotgia, F., Bruno, C., Scartezzini, P., Broda, P., Bado, M., Masetti, E., Mazzocco, P., Egeo, A., Donati, M. A., Volonte, D., Galbiati, F., Cordone, G., Bricarelli, F. D., Lisanti, M. P., and Zara, F. (1998) *Nat. Genet.* **18,** 365–368
28. Galbiati, F., Volonte, D., Minetti, C., Chu, J. B., and Lisanti, M. P. (1999) *J. Biol. Chem.* **274,** 25632–25641
29. Galbiati, F., Volonte, D., Minetti, C., Bregman, D. B., and Lisanti, M. P. (2000) *J. Biol. Chem.* **275,** 37702–37711
30. Scherer, P. E., Tang, Z.-L., Chun, M. C., Sargiacomo, M., Lodish, H. F., and Lisanti, M. P. (1995) *J. Biol. Chem.* **270,** 16395–16401
31. Engelman, J. A., Zhang, X. L., Galbiati, F., and Lisanti, M. P. (1998) *FEBS Lett.* **429,** 330–336
32. Mikel, U. V. (1994) *Advanced Laboratory Methods in Histology and Pathology*, Armed Forces Institute of Pathology/American Registry of Pathology, Washington, D. C.
33. Sargiacomo, M., Sudol, M., Tang, Z.-L., and Lisanti, M. P. (1993) *J. Cell Biol.* **122,** 789–807
34. Lisanti, M. P., Scherer, P. E., Vidugiriene, J., Tang, Z.-L., Hermanoski-Vosatka, A., Tu, Y.-H., Cook, R. F., and Sargiacomo, M. (1994) *J. Cell Biol.* **126,** 111–126
35. Engelman, J. A., Wycoff, C. C., Yasuhara, S., Song, K. S., Okamoto, T., and Lisanti, M. P. (1997) *J. Biol. Chem.* **272,** 16374–16381
36. Koleske, A. J., Baltimore, D., and Lisanti, M. P. (1995) *Proc. Natl. Acad. Sci. U. S. A.* **92,** 1381–1385
37. Franzini-Armstrong, C. (1991) *Dev. Biol.* **146,** 353–63
38. Ioffe, E., Liu, Y., Bhaumik, M., Poirier, F., Factor, S., and Stanley, P. (1995) *Proc. Natl. Acad. Sci. U. S. A.* **92,** 7357–7361
39. Li, S., Galbiati, F., Volonte, D., Sargiacomo, M., Engelman, J. A., Das, K., Scherer, P. E., and Lisanti, M. P. (1998) *FEBS Lett.* **434,** 127–134
40. McNally, E. M., de Sá Moreira, E., Duggan, D. J., Bonnemann, C. G., Lisanti, M. P., Lidov, H. G. W., Vainzof, M., Passos-Bueno, M. R., Hoffman, E. P., Zatz, M., and Kunkel, L. M. (1998) *Hum. Mol. Genet.* **7,** 871–877
41. Doyle, D., Goings, G., Upshaw-Earley, J., Ambler, S., Mondul, A., Palfrey, H., and Page, E. (2000) *Circ. Res.* **87,** 480–488
42. Simons, K., and Ikonen, E. (1997) *Nature* **387,** 569–572
43. Fra, A. M., Williamson, E., Simons, K., and Parton, R. G. (1994) *J. Biol. Chem.* **269,** 30745–30748
44. Brown, D. A., and London, E. (1997) *Biochem. Biophys. Res. Commun.* **240,** 1–7
45. Brown, D. A., and London, E. (1998) *Annu. Rev. Cell Dev. Biol.* **14,** 111–136
46. Sargiacomo, M., Scherer, P. E., Tang, Z.-L., Casanova, J. E., and Lisanti, M. P. (1994) *Oncogene* **9,** 2589–2595
47. Smart, E., Ying, Y.-S., Conrad, P., and Anderson, R. G. W. (1994) *J. Cell Biol.* **127,** 1185–1197
48. Scherer, P. E., Lisanti, M. P., Baldini, G., Sargiacomo, M., Corley-Mastick, C., and Lodish, H. F. (1994) *J. Cell Biol.* **127,** 1233–1243
49. Lisanti, M. P., Tang, Z.-T., Scherer, P., and Sargiacomo, M. (1995) *Methods Enzymol.* **250,** 655–668
50. Schnitzer, J. E., Oh, P., Jacobson, B. S., and Dvorak, A. M. (1995) *Proc. Natl. Acad. Sci. U. S. A.* **92,** 1759–1763
51. Corley-Mastick, C., Brady, M. J., and Saltiel, A. R. (1995) *J. Cell Biol.* **129,** 1523–1531
52. Robbins, S. M., Quintrell, N. A., and Bishop, M. J. (1995) *Mol. Cell. Biol.* **15,** 3507–3515
53. Parton, R. G., Way, M., Zorzi, N., and Stang, E. (1997) *J. Cell Biol.* **136,** 137–154
54. Ishikawa, H. (1968) *J. Cell Biol.* **38,** 51–66
55. Hagiwara, Y., Sasaoka, T., Arashi, K., Imamura, M., Yorifuji, H., Nonaka, I., Ozawa, E., and Kikuchi, T. (2000) *Hum. Mol. Genet.* **9,** 3047–3054

Caveolin-3 Null Mice Show a Loss of Caveolae, Changes in the Microdomain Distribution of the Dystrophin-Glycoprotein Complex, and T-tubule Abnormalities

Ferruccio Galbiati, Jeffrey A. Engelman, Daniela Volonte, Xiao Lan Zhang, Carlo Minetti, Maomi Li, Harry Hou, Jr., Burkhard Kneitz, Winfried Edelmann and Michael P. Lisanti

J. Biol. Chem. 2001, 276:21425-21433.
doi: 10.1074/jbc.M100828200 originally published online March 19, 2001
